Hindawi
Advances in Materials Science and Engineering
Volume 2019, Article ID 8603065, 8 pages
https://doi.org/10.1155/2019/8603065

Research Article

Equation for the Degradation of Uniaxial Compression Stress of Concrete due to Freeze-Thaw Damage

Xiaolin Yang,[1,2] **Genhui Wang**,[1] **Shiwu Gao**,[2] **Min Song**,[3] **and Anqi Wang**[2]

[1]*School of Civil Engineering, Lanzhou Jiaotong University, Lanzhou, Gansu 730070, China*
[2]*School of Civil Engineering, Qinghai University, Xining, Qinghai 810016, China*
[3]*Institute of Applied Mechanics, Taiyuan University of Technology, Taiyuan, Shanxi 030024, China*

Correspondence should be addressed to Genhui Wang; 13609341991@139.com

Received 20 August 2019; Revised 13 October 2019; Accepted 26 November 2019; Published 18 December 2019

Academic Editor: Mohammad A. Hariri-Ardebili

To study the freeze-thaw damage characteristics of concrete, the uniaxial compressive tests of concrete under different number of freeze-thaw cycles were conducted, and the damage variable of freeze-thaw was obtained. The test results showed that the stress was a function of strain and freeze-thaw damage variable, and it can describe the degradation of concrete strength. Meanwhile, the equation for the stress-strain curved surface about strain and freeze-thaw damage variable was also proposed in this paper. The derivative function of the stress-strain curved surface equation with respect to strain presented the change of elastic modulus with the increase of freeze-thaw cycle number. Equation proposed in this paper can be used for predicting the concrete lifetime effectively in cold and large temperature difference regions.

1. Introduction

Due to the cold weather and large temperature difference between day and night in the Qinghai-Tibet Plateau, concrete and prestressed concrete structures are likely to freeze at night and thaw due to solar radiation during the day, operating under frequent freeze-thaw cycles. Freeze-thaw cycling conditions are a primary cause of durability deterioration of concrete structures in the areas with large temperature differences in the Qinghai-Tibet Plateau.

In recent years, many scholars have studied the macroscopic characterization and microscopic mechanism of the mechanical properties of concrete after freeze-thaw cycles. The typical research methods include macroscopic mechanical property and microscopic characterization. Guo [1] summarized and studied the principle of reinforced concrete. He suggested that the compressive stress-strain curve of concrete was a comprehensive and macroscopic response of its mechanical properties and that this relationship was the most basic constitutive relationship in the nonlinear analysis of reinforced concrete structures. Huda and Shahria Alam [2] studied freeze-thaw durability performance of recycled coarse aggregate concrete in accordance with a national standard, and their experimental results showed that the performance of recycled aggregate concrete (RAC) slightly decreased with increasing RCA replacement levels. However, the overall performance was comparable to natural aggregate concrete. Liu and Wang [3] investigated the stress-strain relationship of fly ash concrete after 0, 5, 15, 30, 50, 75, 100, and 125 freeze-thaw cycles by testing 24 prism-shaped specimens. A damage constitutive model based on the damage mechanics and a multiple sharp degradation point model were presented. The proposed model was proven to be effective for evaluating the stress-strain relationship of fly ash concrete under freeze-thaw cycles. Guo and Weng [4] used relative dynamic elastic modulus tests and scanning electron microscopy (SEM) images to study the durability of airport pavement concrete, and their experimental results indicated that the freeze-thaw durability of the concrete coated with surface treatments improved compared with noncoated concrete, and the modified polyurea exhibited good freeze-thaw resistance. Tian et al. [5] used computed tomography (CT) scans and SEM technology to study the erosion degradation behavior

of concrete due to the combined influence of freeze-thaw cycles and sulfate solutions from a microscopic perspective. It was found that the mass loss of the concrete samples increased initially and then decreased slightly. The uniaxial compressive strength increased first and subsequently decreased. Based on the characteristics of the whole stress-strain curve of concrete undergoing different numbers of freeze-thaw cycles, Guan et al. [6] studied the variables that cause damage and established a damage evolution equation for concrete after freeze-thaw cycling. Wang et al. [7] studied the stress-strain relationship of concrete using an ultralow temperature freeze-thaw environment. The experimental results showed that the peak stress during concrete uniaxial compression decreased with the increase in the number of freeze-thaw cycles for ultralow temperature freeze-thaw cycling, whereas the peak strain increased and the stress-strain curve decreased.

In this paper, the microscopic pore structure characteristics of concrete were measured using SEM during the freeze-thaw cycling of air-freezing and water-thawing, and the variation of the microcracks and void ratio were analyzed quantitatively. The stress-strain curve of concrete with different numbers of freeze-thaw cycles was measured. A freeze-thaw damage variable related to modified Loland damage model was proposed in this paper. Based on the four stress-stain curves, the equation for the stress-strain curved surface about strain and freeze-thaw damage variable were determined, and the evolution of the elastic modulus during freeze-thaw cycles was discussed.

2. Materials and Methods

The superstructures of concrete bridges in Qinghai-Tibet Plateau are mainly composed of C40 concrete. Based on the mixture ratio recommended in the literature [8] (Table 1), eight groups of cubic specimens with dimensions of 100 mm × 100 mm × 100 mm were poured with Shuoshan PO.42.5 ordinary Portland cement from Datong County, Qinghai Province, China. After 28 d in the standard curing room, the samples were used for quasi-static compression and splitting tension tests.

The freeze-thaw test of the concrete followed the slow freezing method stipulated in the "Standard for Testing Method of Long-term Performance and Durability of Ordinary Concrete" [9]. Before freezing and thawing, the specimens were immersed in water for 4 d, after which they were placed in a freezer at −18°C for no less than 4 h. After freezing, the melting time should be no less than 4 h after water at 20°C was added. During the freeze-thaw process, a thermocouple was used to measure the center temperature of the test block to ensure that the center temperature of the test block reached the freeze-thaw temperature. The numbers of freeze-thaw cycles of the concrete blocks were 0, 25, 50, and 75. The microstructure of the concrete included aggregate, hydrated cement paste, and an interface transition zone between the cement paste and aggregate [10]. In this study, the micromorphology of the concrete after freeze-thaw cycling was observed by means of high-resolution SEM (JSM-6610LV).

Table 1: Mix proportions of concrete.

Elements	Cement	Water	Sand	Gravel
Material content (kg/m^3)	388	190	601	1221
Ratio of weight	1	0.49	1.55	3.15

The compression of the concrete cubes was based on a test method standard for determining the mechanical properties of ordinary concrete [11]. The full stress-strain curves of concrete subjected to different numbers of freeze-thaw cycles were measured using a HUT1000k computer-controlled hydraulic universal testing machine manufactured by Shenzhen Wance Experimental Equipment Co. Ltd. Displacement loading mode was adopted in the experiment, and the loading rate was 1 mm/min. Data processing was conducted based on the requirements of the standard test method for the mechanical properties of ordinary concrete. According to this standard, the measured strength values of the 100 mm × 100 mm × 100 mm specimens must be multiplied by a dimension conversion coefficient of 0.95 [11].

3. Results

3.1. Micropore Structure under Freeze-Thaw Cycles. Figures 1(a), 1(c), 1(e), and 1(g) show the microstructures of the hydrated cement pastes observed using SEM with 500x magnification. With the increase in the number of freeze-thaw cycles, the micropore structure developed gradually, and microcracks formed after 75 freeze-thaw cycles. Figures 1(b), 1(d), 1(f), and 1(h) show binary diagrams of the micropore structures of the concrete analyzed by the pore and crack image identification and analysis system (PCAS) [12, 13]. With the increase in the number of freeze-thaw cycles, the percentage of microcracks and micropores in the concrete gradually increased from 2.74% to 10.83% after 75 freeze-thaw cycles. Generally, the number of cracks and micropores increased during the freeze-thaw cycling.

3.2. Compressive Properties of Concrete. During the quasi-static compression tests, the stress-strain curves of the concrete blocks subjected to 0, 25, 50, and 75 freeze-thaw cycles were measured (Figure 2). During the displacement loading tests, the peak stress corresponding to the stress-strain curve decreased gradually, whereas the peak strain increased gradually, and the compressive stress-strain full curve had a tendency to shift downward and to the right. The peak stress and peak strain values of the typical stress-strain curves of each group are shown in Table 2. The peak stress of the unfrozen-thawed concrete was 44.93 MPa, and the value of the peak strain was 2150.3 $\mu\varepsilon$, which was close to the value given by the FIP Model Code (2010) specification [14]. When the graded concrete had a strain of 2%, the average compressive strength was 48 MPa. The variation of the quasi-static stress-strain curve with the number of freeze-thaw cycles was consistent with that reported previously [7]. As the number of freeze-thaw cycles increased, the peak stress of the concrete decreased, the peak strain increased, the number of internal microcracks and pores increased, and

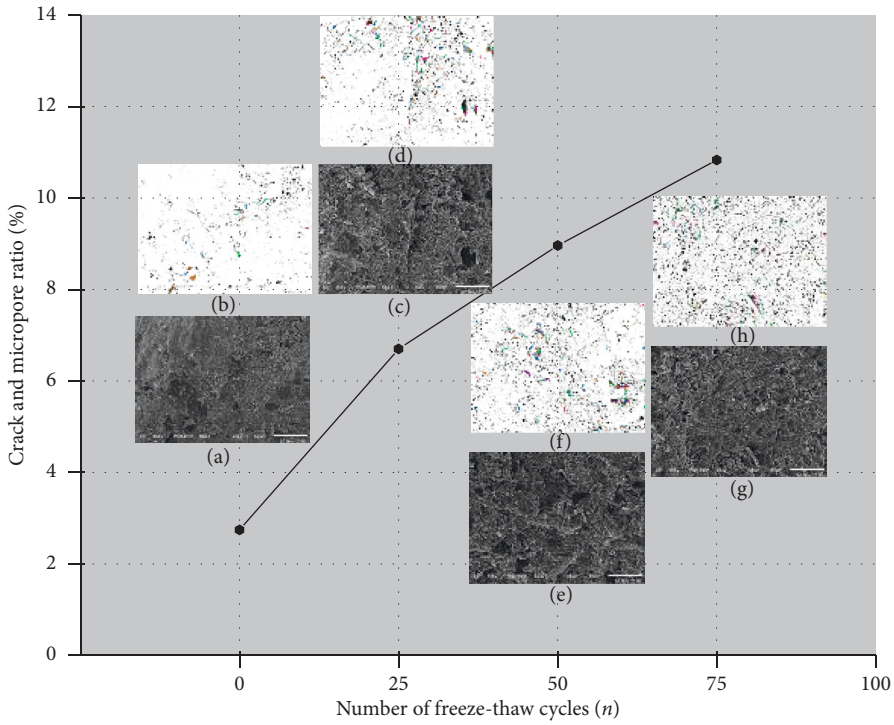

Figure 1: Micropore structure growth behavior for specimen (SEM 500x). (a) FTC00. (b) Binary diagram for FTC00. (c) FTC25. (d) Binary diagram for FTC25. (e) FTC50. (f) Binary diagram for FTC50. (g) FTC75. (h) Binary diagram for FTC75.

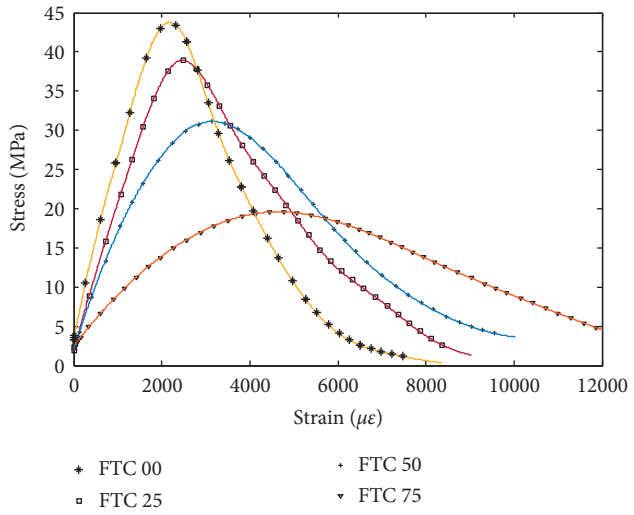

Figure 2: Full uniaxial compression stress-strain curves of concrete after different freeze-thaw cycling.

Table 2: Quasi-static compression test results of concrete after different numbers of freezing-thaw cycles.

Number of freeze-thaw cycles	f_{cm} (MPa)	ε_{cm} (10^{-6})	ε_{cm} (10^{-6}) (model code 2010)
0	44.93	2150.3	2400
25	40.10	2482.0	—
50	31.57	3095.0	—
75	19.67	4696.7	—

Note. f_{cm} is the peak stress and ε_{cm} is the strain at peak stress.

the pore size increased; these results agreed with those reported previously [8]. The peak stress of the concrete under uniaxial compression decreased, and the peak strain increased.

4. Discussion

4.1. Freeze-Thaw Damage Variable. Many studies had been conducted and some damage models were proposed by

researchers [15, 16]. Among these models, Loland damage model was considered as an effective method to study the damage in concrete [17]. Based on the macroscopic phenomenological theory, the Loland damage model mainly considered the influence of damage on the macroscopic mechanical properties of materials. In order to study the damage evolution in freeze-thaw cycles, a modified Loland damage model was proposed by Cai [18]. In this paper, the model from [18] was used to describe the damage law of concrete peak compressive strength about the number of freeze-thaw cycles. The relative dynamic elasticity modulus was used to evaluate the damage situation. And, the ratio of the peak compressive strength for different freeze-thaw numbers to the concrete strength without freeze-thaw was also used to describe damage circumstance [19].

Generally, an isotropic scalar D can be used to indicate the damage degree of concrete after freeze-thaw cycles, and the value was in the interval of [0, 1]. When $D = 0$, the material was not damaged, and when $D = 1$, the material was damaged completely. The damage variable can be expressed as follows:

$$D = D_0 + C_1\left(\frac{n}{N}\right)^{\beta}, \tag{1}$$

where n is the number of freeze-thaw cycles and N is the freeze-thaw lifetime, which was assumed to be 100 in this study ($N = 100$). D_0 is the initial damage, and its value is set to be zero ($D_0 = 0$). C_1 and β are parameters related to peak compressive strength for concrete under different freeze-thaw cycles. And, the values of C_1 and β were 1.03 and 1.258, respectively. Then, the freeze-thaw damage variable is illustrated as follows:

$$D = 1.03 \times \left(\frac{n}{100}\right)^{1.258}. \tag{2}$$

The increase in trend of damage variable versus different number of freeze-thaw cycles is shown in Figure 3(a). In order to verify the effectiveness of equation (2), the damage variable was calculated by two ways. The number of freeze-thaw cycles, elastic modulus, and peak compressive strength were obtained from [20], and then the corresponding values of C_1 and β were acquired. Meanwhile, the ratio of the error between initial elastic modulus and the elastic modulus for different freeze-thaw number to initial elastic modulus was obtained to evaluate the damage variable values. And, the values of damage variable are shown in Figure 3(b). The well agreement between the values from two methods was found. Thus, the correctness for the method proposed in this paper was verified.

The four uniaxial compressive stress-strain curves of concrete subjected to different freeze-thaw cycles can be plotted in a three-dimensional coordinate system (Figure 4) with the freeze-thaw damage variable as one of the independent variables.

The stress-strain relationship of concrete subjected to 0, 25, 50, and 75 freeze-thaw cycles can be clearly expressed in the stress space with the freeze-thaw damage factor as the Y-axis. The ascending and descending sections were steeper for the undamaged specimen curve than those of the damaged specimen curves. As shown in Figure 1, the microscopic pore structure grew, which caused the concrete to become looser and spalled. At the macroscopic level, the microstructures, which included micropores and microcracks, tended to close under compression, resulting in a decrease in the slope of the ascending section of the stress-strain curve and a flattening of the overall curve [21].

4.2. Stress-Strain Curved Surface Equation of Concrete after Freezing and Thawing. To account for the influence of the freeze-thaw cycling and evaluate the stress-strain constitutive relation associated with the freeze-thaw damage variable, a 2D rational function (equation (3)) and Levenberg–Marquardt optimization algorithm [22] were employed. Defining the vector $\mathbf{A} = [a_1, a_2, a_3, a_4]$ as the coefficient matrix of the strain and vector $\mathbf{B} = [b_1, b_2, b_3, b_4, b_5]$ as the coefficient matrix of the freeze-thaw damage variable, the rational function was defined as follows:

$$\sigma_{(\varepsilon,D)} = \frac{a_1\varepsilon + b_1 D + b_2 D^2 + b_3 D^3}{1 + a_2\varepsilon + a_3\varepsilon^2 + a_4\varepsilon^3 + b_4 D + b_5 D^2}, \tag{3}$$

where D is the freeze-thaw damage variable in a freeze-thaw cycle, ε is the strain, and σ is the stress.

Using the experimental data, the damage evolution equation due to concrete freeze-thaw cycling can be expressed as follows:

$$\begin{cases} \sigma_{(\varepsilon,D)} = \dfrac{0.019\varepsilon - 1.89\,D + 124.36D^2 - 106.3D^3}{1 - 0.00024\varepsilon + 1.79 \times 10^{-8}\varepsilon^2 + 4.08 \times 10^{-11}\varepsilon^3 + 0.417\,D + 4D^2}, \\ R^2 = 0.85, \end{cases} \tag{4}$$

where R^2 is the coefficient for the fitted function.

The influence of the strain and freeze-thaw damage variable on the concrete stress strength was captured by equation (4). Combining equation (2) and equation (4), the concrete stress about strain and the number of freeze-thaw cycles were obtained under uniaxial compression. The stress surfaces are plotted in Figure 5. Figure 5(a) shows the curved surface drawn by fitting the data, and Figure 5(b) shows a curved surface drawn using the Wolfram Mathematica software based on equation (4). The unit of strain in the figures was microstrain (10^{-6}), the freeze-thaw damage variable was a dimensionless quantity with values between 0 and 1, and the unit of stress was MPa.

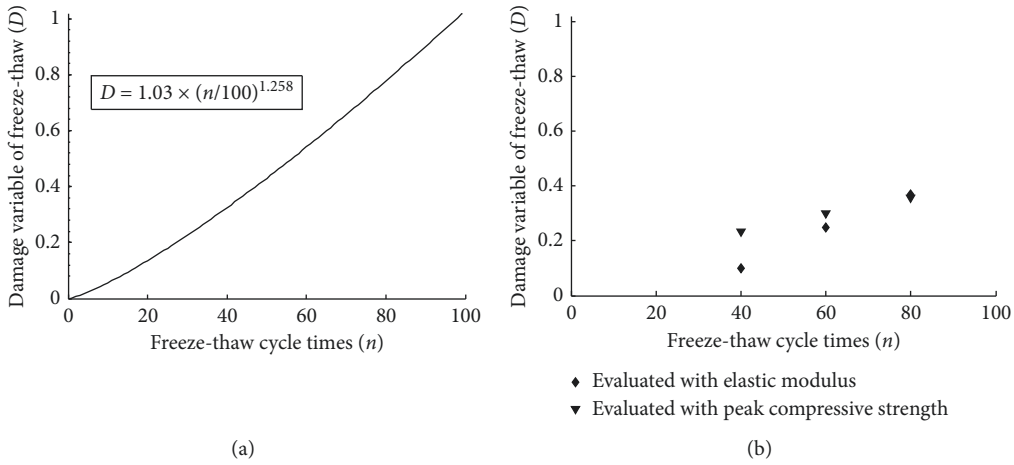

Figure 3: Damage variable versus freeze-thaw cyclic times: (a) experiment results; (b) comparison between two methods based on [20].

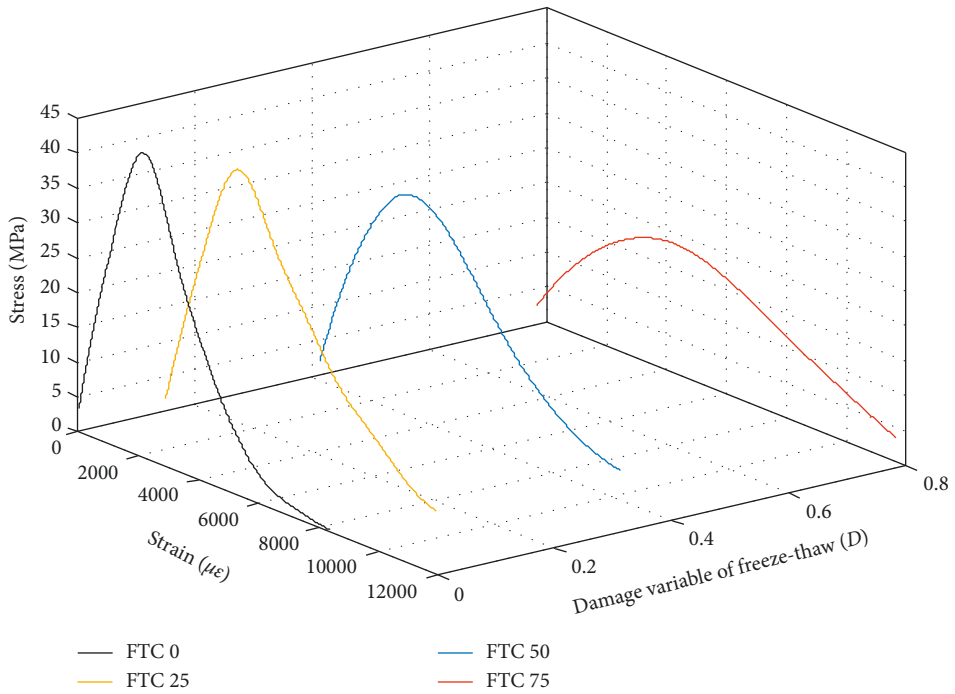

Figure 4: Uniaxial compression stress-strain curves in a three-dimensional coordinate system.

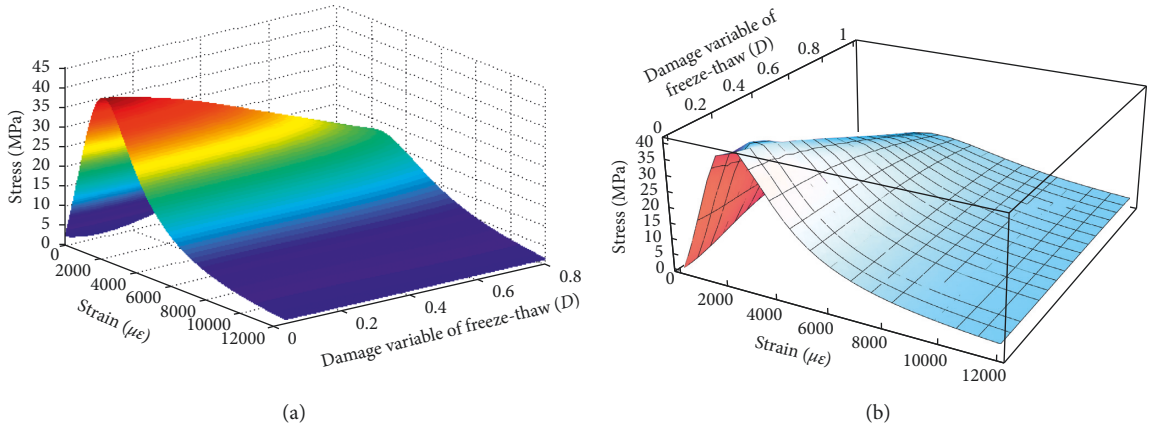

Figure 5: Full stress-strain surface with freeze-thaw damage variable. (a) Drawn by fitting the data. (b) Drawn using equation (4).

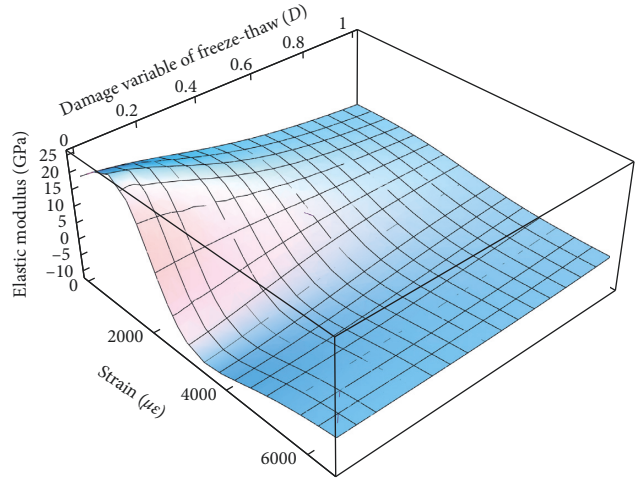

Figure 6: Stress-strain surface with varying freeze-thaw damage variable and elastic modulus surface.

Table 3: Quasi-static compression test data and elastic modulus after different numbers of freeze-thaw cycles.

Number of freeze-thaw cycles	f_{cm} (MPa)	ε_{cm} (10^{-6})	D	E_0 (GPa)	E_{max} (GPa)	E_c (GPa)
0	44.93	2150.3	0.003	13.6	23.5	35.5
25	40.10	2482.0	0.115	12.8	21.9	34.2
50	31.57	3095.0	0.267	9.7	12.4	31.5
75	19.67	4696.7	0.502	4.4	4.6	26.9

Note. f_{cm} is the peak stress, ε_{cm} is the strain at peak stress, E_0 is the initial tangential elastic modulus, E_{max} is the maximum tangential elastic modulus, and E_c is the elastic modulus estimated by the FIP Model Code (2010) in dry state.

4.3. Application for Stress-Strain Curved Surface Equation. The mass loss rate, dynamic elastic modulus, peak stress, and peak strain were commonly used to indicate the stress-strain relationship of concrete after freezing and thawing. Studies have shown that the dynamic elastic modulus was significantly reduced with the expansion of the microscopic pore structure inside the concrete during freeze-thaw cycles [23]. Meanwhile, the peak stress decreased and the peak strain increased [24]. By finding the partial derivative of the stress corresponding to the change in equation (4), the distribution of elastic modulus for each point in the stress-strain space was obtained as follows:

$$E_{(\varepsilon,D)} = \frac{\partial \sigma}{\partial \varepsilon} = \frac{190}{1 - 0.00024\varepsilon + 1.79 \times 10^{-8}\varepsilon^2 + 4.08 \times 10^{-11}\varepsilon^3 + 0.417\,D + 4D^2} - \frac{\left(-0.24 + 3.58 \times 10^{-5}\varepsilon + 1.223 \times 10^{-7}\varepsilon^2\right)\left(0.019\varepsilon - 1.89\,D + 124.36D^2 - 106.3D^3\right)}{\left(1 - 0.00024\varepsilon + 1.79 \times 10^{-8}\varepsilon^2 + 4.08 \times 10^{-11}\varepsilon^3 + 0.417\,D + 4D^2\right)^2}. \quad (5)$$

The dimensions and units of the quantities in the above formula were the same as those in equation (4).

Equation (5) was used to calculate the change in the tangential elastic modulus. And, Figure 6 shows the surfaces plotted with equations (5) in the 0–6500 microstrain range, 0–1.0 freeze-thaw damage range. The tangential elastic modulus of concrete can be divided into the following stages as the strain changes: (a) during the ascending section of the stress-strain curve, the tangential elastic modulus first increased and subsequently decreased, and the elastic modulus reached the peak value within the first 1/2–2/3 of the ascending section of the curve; (b) at the peak stress, the value of the elastic modulus was close to 0; and (c) in the descending section of the stress-strain curve, the elastic modulus was negative.

The values of elastic modulus computed from equation (4) and the FIP Model Code (2010) for 0, 25, 50, and 75 freeze-thaw cycles are shown in Table 3.

The formula for the elastic modulus of ordinary concrete specified by the FIP Model Code (2010) is as follows:

$$E_c = 2.15 \times 10^4 \left(\frac{f_{cm}}{10}\right)^{1/3}, \quad (6)$$

where E_c is the elasticity modulus of concrete (MPa) and f_{cm} is the average value of the compressive strength (MPa).

The three elastic moduli (initial tangential, maximum tangential, and estimated elastic moduli) shown in Table 3 are in the same order of magnitude, and E_{max} and E_0 were

small than the value of E_c, which resulted that the elastic modulus of concrete in the saturated state was lower than the value in the dry state [20].

5. Conclusions

SEM images and macromechanical properties were used to study the damage of concrete due to freeze-thaw cycling. The stress-strain curves under uniaxial compression were discussed in detail. The main conclusions were summarized as follows.

The microcracks and pores in the concrete increased with the increase of freeze-thaw cycles. During the freeze-thaw process, the periodic reciprocating stress around the internal microporosity structure made the internal damage accumulate gradually. With the increase in the number of freeze-thaw cycles, the peak stress of the concrete under uniaxial compression decreased gradually, while the strain corresponding to the peak stress increased.

The modified Loland damage model was used to evaluate the mechanical behavior of the freeze-thaw damage. The damage evolution variable could express the damage evolution behavior of the concrete. Based on the stress-strain full curve of concrete under the different number of freeze-thaw cycles, the stress-strain curved surface equation was proposed.

The value of elastic modulus predicted from the equation in this paper agrees well with the value in FIP Model Code (2010). And, the equation can help predict the mechanical properties for major engineering structure in the cold region.

Data Availability

All experimental data, models, and code generated or used during the study are available from the corresponding author upon request.

Conflicts of Interest

The authors declare that there are no conflicts of interest regarding the publication of this paper.

Acknowledgments

This work was supported by the National Natural Science Foundation of China (no. 11472146) and the Science and Technology Projects of Qinghai Province, PRC (nos. 2016-ZJ-721 and 2017-ZJ-783).

References

[1] Z. Guo, *Principles of Reinforced Concrete*, Elsevier, Amsterdam, Netherlands, 2014.

[2] S. B. Huda and M. Shahria Alam, "Mechanical and freeze-thaw durability properties of recycled aggregate concrete made with recycled coarse aggregate," *Journal of Materials in Civil Engineering*, vol. 27, no. 10, Article ID 04015003, 2015.

[3] M.-H. Liu and Y.-F. Wang, "Damage constitutive model of fly ash concrete under freeze-thaw cycles," *Journal of Materials in Civil Engineering*, vol. 24, no. 9, pp. 1165–1174, 2012.

[4] T. Guo and X. Weng, "Evaluation of the freeze-thaw durability of surface-treated airport pavement concrete under adverse conditions," *Construction and Building Materials*, vol. 206, pp. 519–530, 2019.

[5] W. Tian, X. Li, and F. Wang, "Experimental study on deterioration mechanism of concrete under freeze-thaw cycles coupled with sulfate solution," *Bulletin of the Chinese Ceramic Society*, vol. 38, no. 3, pp. 119–127, 2019.

[6] X. Guan, D. Niu, J. Wang, and L. Jiang, "Study on freeze-thaw damage constitutive model of concrete considering plastic strain and damage threshold," *Journal of Disaster Prevention and Mitigation Engineering*, vol. 35, no. 6, pp. 777–784, 2015.

[7] X. Wang, J. Xie, P. Li, and X. Li, "Experimental study on complete stress-strain curve of concrete after freeze-thaw cycles under extra-low temperatures," *Water Resources and Hydropower Engineering*, vol. 45, no. 8, pp. 159–164, 2014.

[8] B. Zhang, *Concrete and Mortar Mixing Ratio Manual*, Tianjin University Press, Tiasnjin, China, 2012.

[9] China Academy of Building Research, *Standard Test Method for Long-Term Performance and Durability of Ordinary Concrete GB/T50082-2009*, China Architecture & Building Press, Beijing, China, 2010.

[10] P. K. Mehta and P. J. M. Monteiro, *Concrete: Microstructure, Properties, and Materials*, McGraw Hill Professional, New York, NY, USA, 2013.

[11] China Academy of Building Research, *Standard Test Method for Mechanical Properties of Ordinary Concrete GB/T 50081-2002*, China Architecture & Building Press, Beijing, China, 2004.

[12] C. Liu, C.-S. Tang, B. Shi, and W.-B. Suo, "Automatic quantification of crack patterns by image processing," *Computers & Geosciences*, vol. 57, pp. 77–80, 2013.

[13] C. Liu, B. Shi, J. Zhou, and C. Tang, "Quantification and characterization of microporosity by image processing, geometric measurement and statistical methods: application on SEM images of clay materials," *Applied Clay Science*, vol. 54, no. 1, pp. 97–106, 2011.

[14] Fib, *Fib Model Code for Concrete Structures 2010*, International Federation for Structural Concrete (Fib), Lausanne, Switzerland, 2010.

[15] A. Duan, Y. Tian, J.-G. Dai, and W.-L. Jin, "A stochastic damage model for evaluating the internal deterioration of concrete due to freeze–thaw action," *Materials and Structures*, vol. 47, no. 6, pp. 1025–1039, 2014.

[16] Y.-L. Chen, J. Ni, L.-H. Jiang, M.-L. Liu, P. Wang, and R. Azzam, "Experimental study on mechanical properties of granite after freeze–thaw cycling," *Environmental Earth Sciences*, vol. 71, no. 8, pp. 3349–3354, 2014.

[17] N. Gong and X. Liu, "Concrete failure criterion under freeze-thaw condition in structural engineering," *Sichuan Building Science*, vol. 31, no. 6, pp. 144–147, 2005.

[18] H. Cai, *Prediction Model of Concrete Freeze-Thaw Durability*, Tsinghua University, Beijing, China, 1998.

[19] A. Chen, Q. Zhang, J. Wang, and Z. Gai, "Freeze-thaw cycle test and a damage mechanics model for recycled concrete," *Engineering Mechanics*, vol. 26, no. 11, pp. 102–107, 2009.

[20] W. Tian, K. Xing, and Y. Xie, "Experimental study of concrete of damage degradation mechanism in freeze-thaw environment," *Journal of Experimental Mechanics*, vol. 30, no. 3, pp. 299–304, 2015.

[21] J. Wu, X. Jing, and Z. Wang, "Uni-axial compressive stress-strain relation of recycled coarse aggregate concrete after freezing and thawing cycles," *Construction and Building Materials*, vol. 134, pp. 210–219, 2017.

[22] P. L. Gould and Y. Feng, *Introduction to Linear Elasticity*, Springer, Basel, Switzerland, 2018.

[23] J. Zhang, X. Weng, L. Jiang, B. Yang, and J. Liu, "Frost resistance of concrete reinforced using surface-strengthening materials in airport pavements," *Journal of Materials in Civil Engineering*, vol. 30, no. 3, Article ID 04018006, 2018.

[24] X. Guan, J. Qiu, H. Song, Q. Qin, and C. Zhang, "Stress–strain behaviour and acoustic emission characteristic of gangue concrete under axial compression in frost environment," *Construction and Building Materials*, vol. 220, pp. 476–488, 2019.